Supporting Information

Rapid Accessible Fabrication and Engineering of Bilayered Hydrogels: Revisiting the Cross-Linking Effect on Superabsorbent Poly(acrylic acid)

Kyoung Min Lee,[†,‡] Hea Ji Kim,[†] Doyoung Jung,[†] Yuree Oh,[†] Hyemin Lee,[§] Changsun Han,[§] Ji Young Chang,*[,‡] and Hyungwoo Kim*[,†]

[†]School of Polymer Science and Engineering, Chonnam National University, Gwangju 61186, Korea
[‡]Department of Materials Science and Engineering, College of Engineering, Seoul National University, Seoul 08826, Korea
[§]Basic Materials and Chemicals R&D, LG Chem, Ltd / R&D Campus Daejeon, 188 Moonji-ro, Yuseong-gu, Daejeon 34122, Korea

*Corresponding author e-mails: kimhw@jnu.ac.kr; jichang@snu.ac.kr

Contents

Effect of Initiator Concentrations on the Mechanical Strength

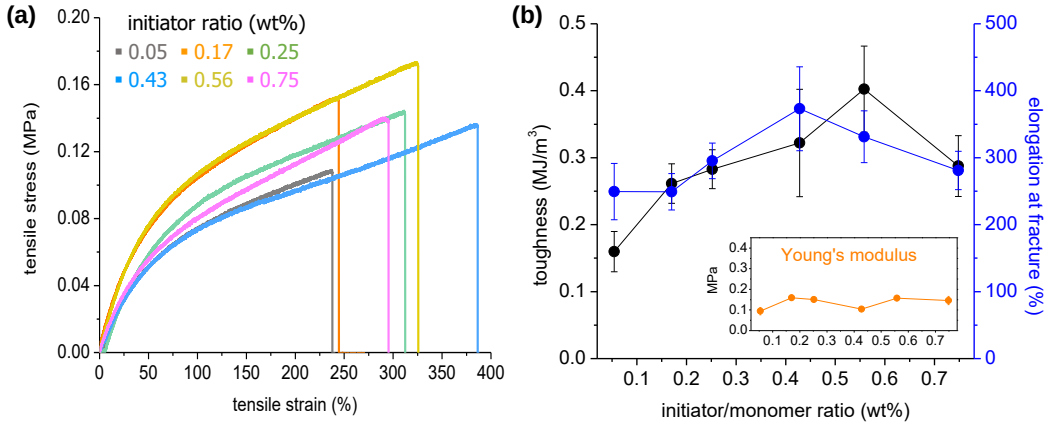

Figure S1. Mechanical properties of hydrogels obtained with different amounts of KPS. (a) Representative tensile stress–strain curves from hydrogels that contain different concentrations of initiator with 0.34 wt% cross-linker. (b) Change in toughness (black) and elongation at fracture (blue) of the hydrogels with respect to the concentration of initiator. Young's modulus (red) was almost maintained as shown in the inset in b. The data points were obtained in quintuplicate from five independent experiments.

Table S1. Average Young's modulus, elongation at fracture, and toughness that correspond to Figure S1b, and 5c.

initiator (wt%)	Young's modulus (MPa)		elongation at fracture (%)		toughness (MJ/m^3)	
	Avg.	Std.	Avg.	Std.	Avg.	Std.
0.05	0.09	0.02	249.4	42.1	0.16	0.03
0.17	0.16	0.01	249.1	27.2	0.26	0.03
0.25	0.15	0.01	295.2	26.5	0.28	0.03
0.43	0.10	0.01	373.1	62.6	0.32	0.08
0.56	0.16	0.01	331.3	38.8	0.40	0.06
0.75	0.15	0.02	280.9	28.6	0.29	0.05

Table S2. Average Young's modulus, elongation at fracture, and toughness that correspond to Figure 4b.

hydrogel film	cross-linker (wt%)	Young's modulus (MPa)		elongation at fracture (%)		toughness (MJ/m^3)	
		Avg.	Std.	Avg.	Std.	Avg.	Std.
1	0.20	0.12	0.01	219.8	40.2	0.17	0.04
2	0.34	0.15	0.01	295.2	26.9	0.28	0.03
3	0.42	0.12	0.01	303.4	24.4	0.27	0.03
4	0.50	0.15	0.01	244.6	36.7	0.25	0.04
5	0.63	0.12	0.01	192.0	14.1	0.14	0.02
6	0.80	0.11	0.01	92.5	14.5	0.04	0.02

Measurement of Mechanical Strengths at Various Temperatures

To test mechanical properties of hydrogel films at high temperature, we used universal testing machine with temperature controlled chamber. Specimens were prepared in way that previously mentioned. Sample specimens were stretched on temperature controlled chamber (40 ℃, 60 ℃, and 80 ℃) until the samples were broken. Furthermore, specimens were left in the chamber and heated for certain time (0 min, 3min, and 10min). Photographs of universal tensile machine when heating to 80 ℃ is shown in Figure S2a.

Table S3. Average Young's modulus, elongation at fracture, and toughness that correspond to Figure 5a–5c.

hydrogel film	cross-linker (wt%)	Temp.	Young's modulus (MPa)		elongation at fracture (%)		toughness (MJ/m^3)	
			Avg.	Std.	Avg.	Std.	Avg.	Std.
1	0.20	25 ℃	0.12	0.01	221.2	36.0	0.17	0.04
3	0.42		0.12	0.01	304.0	22.6	0.27	0.03
6	0.81		0.11	0.01	92.2	12.7	0.04	0.02
1	0.20	80 ℃	0.28	0.05	158.9	34.0	0.63	0.11
3	0.42		0.27	0.06	153.5	35.7	0.29	0.10
6	0.81		0.51	0.07	114.6	23.5	0.35	0.08

Table S4. Average Young's modulus (MPa) of **3** measured at 40 ℃, 60 ℃, and 80 ℃, corresponding to Figure 5d.

exposure time (min)	40 ℃		60 ℃		80 ℃	
	Avg.	Std.	Avg.	Std.	Avg.	Std.
0	0.15	0.01	0.15	0.01	0.15	0.01
3	0.20	0.03	0.28	0.06	0.39	0.13
10	0.35	0.20	0.44	0.21	0.49	0.11

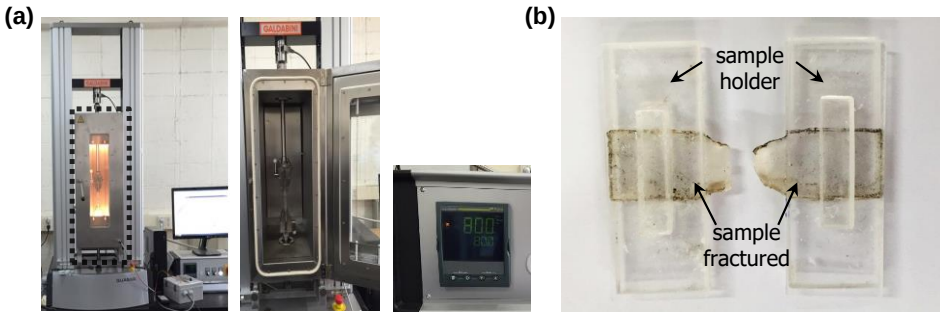

Figure S2. (a) Photographs of universal tensile machine when heating to 80 ℃. (b) Photograph of the hydrogel film **3** containing 0.42 wt% cross-linker after fractured at 80 ℃. Edges were slightly blackened while cutting the pristine film by a laser cutter, which did not affect the tensile strength.

Physical Properties of Bilayered Hydrogels

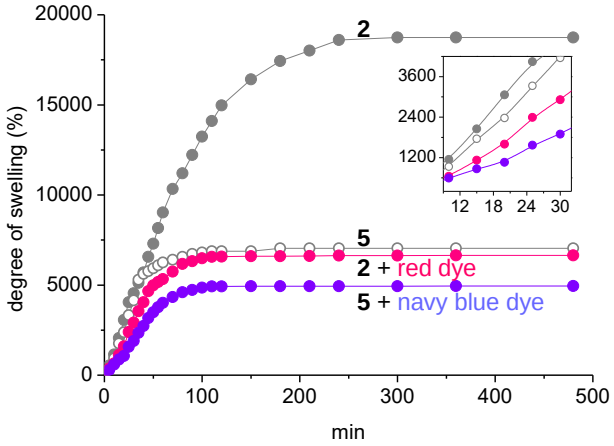

Figure S3. Change in degree of swelling of control layers (red **2** and navy blue **5**). Swelling behaviors of pristine **2** and **5** are shown for comparison. The rate of swelling for red **2** is 114% min^{-1} and navy blue **5**, 65% min^{-1} calculated from the initial linear region shown in the inset.

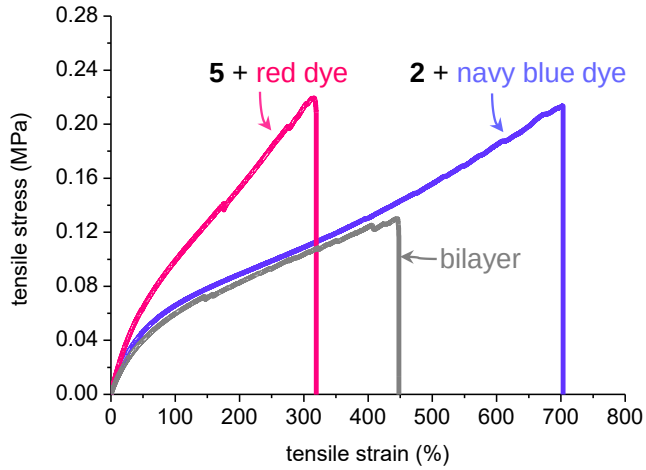

Figure S4. Representative tensile stress–strain curves measured from navy blue **2**, red **5**, and the resulting bilayer.

Table S5. Average Young's modulus, elongation at fracture, and toughness that correspond to Figure 6c.

hydrogel film	Young's modulus (MPa)		elongation at fracture (%)		toughness (MJ/m^3)	
	Avg.	Std.	Avg.	Std.	Avg.	Std.
2	0.15	0.01	295.2	26.9	0.28	0.03
5	0.12	0.01	192.0	14.1	0.14	0.02
navy blue **2**	0.09	0.01	688.0	46.5	0.79	0.06
red **5**	0.14	0.01	334.0	23.0	0.43	0.04
bilayer	0.09	0.00	451.9	31.1	0.39	0.04

Figure S5. Time-lapsed photographs of the bending of the hydrogel bilayer (length, 2.8 cm; width, 0.3 cm; thickness, 2 mm) in a pH 7 buffer solution at 25 ℃, taken every minute. The bilayer was curled into a round within 15 min.

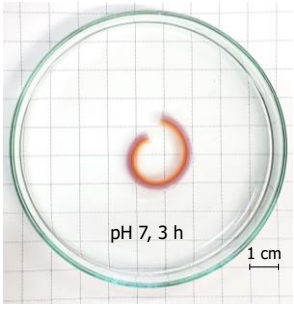

Figure S6. Photograph of the hydrogel bilayer (length, 2.8 cm; width, 0.3 cm; thickness, 2 mm) taken after exposure to a pH 7 buffer solution at 25 ℃ for 3 h.

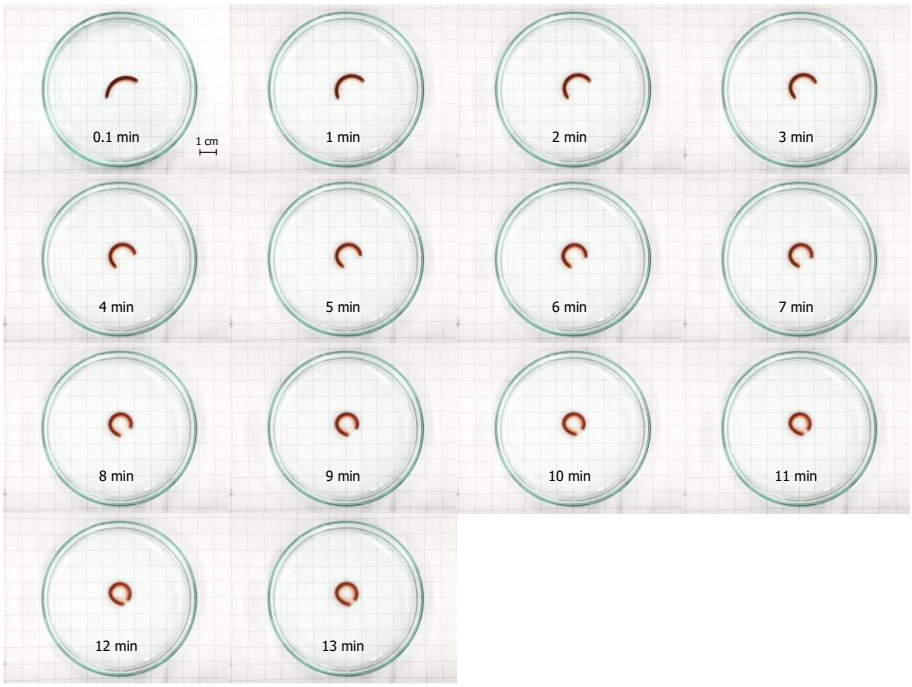

Figure S7. Time-lapsed photographs of the bending of the hydrogel bilayer (length, 2.8 cm; width, 0.3 cm; thickness, 2 mm) in a pH 3 buffer solution at 25 ℃, taken every minute. The bilayer was curled into a round within 13 min.

Figure S8. Time-lapsed photographs of the bending of the hydrogel bilayer (length, 2.8 cm; width, 0.3 cm; thickness, 2 mm) in a pH 10 buffer solution at 25 ℃, taken every minute. The bilayer was curled into a round within 11 min.

Table S6. Change in curvature of bilayered hydrogel in pH 3, 7, and 10 as time elapsed corresponding to Figure 6e.

time (min)	curvature (m^{-1})		
	pH 3	pH 7	pH 10
0.1	82	66	105
1	110	98	142
2	136	117	169
3	144	129	183
4	161	137	196
5	168	148	200
6	172	157	209
7	183	164	216
8	189	174	225
9	190	182	224
10	191	187	224
11	193	195	224
12	190	199	
13	190	204	
14		208	
15		208	

Table S7. Change in degree of swelling of hydrogels **2**, navy blue **2**, red **2**, **5**, navy blue **5**, and red **5** in DI water as time elapsed corresponding to Figure 6b and Figure S3.

time (min)	**2**	navy blue **2**	red **2**	**5**	navy blue **5**	red **5**
0	0	0	0	0	0	0
5	530	341	360	360	279	246
10	1146	784	646	932	592	566
15	2052	1479	1122	1757	866	1137
20	3059	2570	1598	2376	1062	1440
25	4045	3442	2392	3329	1571	2013
30	4538	4342	2916	4154	1897	2413
35	5117	5362	3551	5297	2341	2823
40	5697	5965	4043	5614	2733	3053
45	6567	6544	4662	5773	3164	3233
50	7291	7100	4979	5932	3490	3316
55	8161	7472	5170	6090	3764	3336
60	9030	7822	5329	6249	4012	3373
70	10335	8203	5741	6408	4339	3438
80	11204	8533	6170	6567	4600	3448
90	12219	8771	6329	6725	4730	3516
100	13233	8842	6487	6805	4861	3518
110	14103	8850	6567	6884	4926	3536
120	14972	8900	6583	6884	4926	3556
150	16422	8933	6598	6884	4939	3695
180	17436	9000	6598	7043	4939	3700
210	18016	9017	6614	7043	4939	3718
240	18596	9033	6630	7043	4939	3755
300	18741	9033	6630	7043	4939	3791
360	18741	9067	6646	7043	4952	3791
480	18741	9183	6646	7043	4952	3809

References

1. Ma, J.; Lee, J.; Han, S. S.; Oh, K. H.; Nam, K. T.; Sun, J. Y. Highly Stretchable and Notch-Insensitive Hydrogel Based on Polyacrylamide and Milk Protein. *ACS Appl. Mater. Interfaces.* **2016**, *8*, 29220−29226.

NMR Spectra

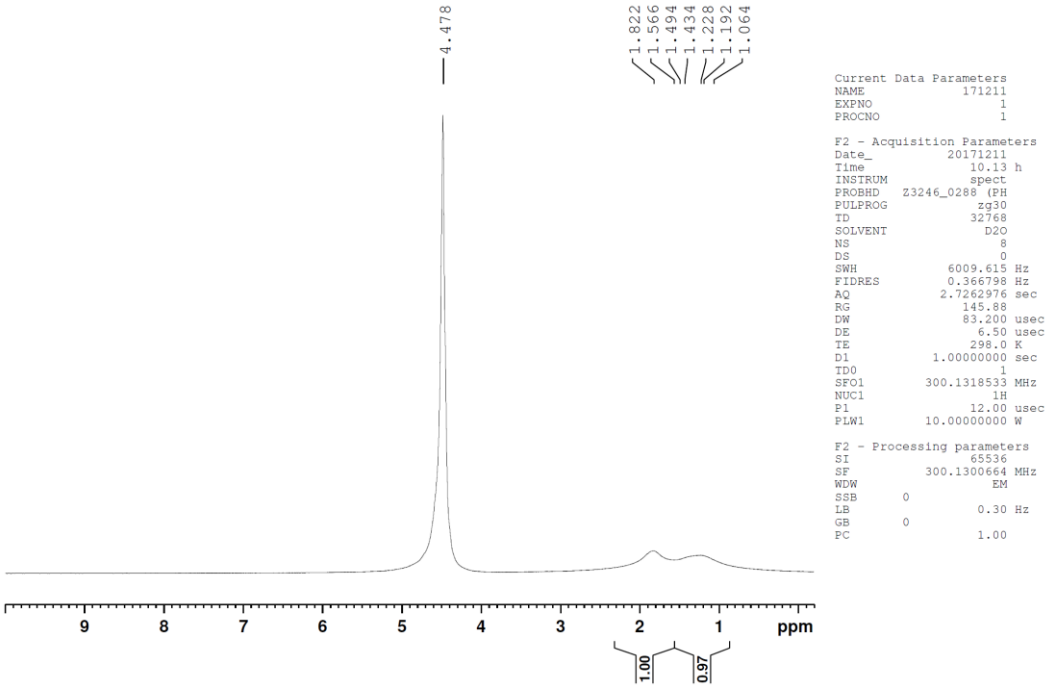

Figure S9. ^{1}H NMR spectrum of **2**.

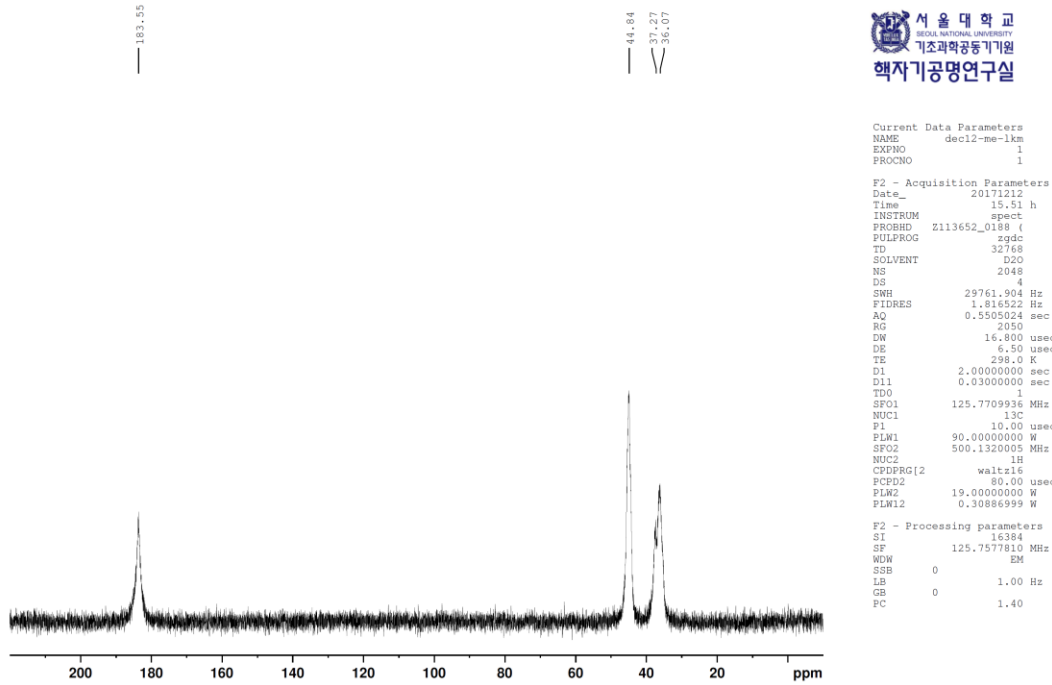

Figure S10. ^{13}C NMR spectrum of **2**.